Multiple Jets Exhausting into a Crossflow

H. ZIEGLER* AND P. T. WOOLER†
Northrop Corporation, Aircraft Division, Hawthorne, Calif.

An analytical model for the flow of a jet exhausting normally into a crossflow has been generalized. The continuity and momentum equations are solved for the jet path and then the velocity field induced by the jet is evaluated by replacing the jet with a sink-doublet singularity distribution, accounting for the entrainment of mainstream fluid and the blockage effect of the jet. For a multiple jet configuration, the influence of an upstream jet on a downstream jet is represented by a reduced mainstream velocity in the equations of motion. Continuity and momentum considerations yield initial conditions for resultant jets after intersection. Good agreement between theory and available experimental data on jet centerlines and surface pressure distributions is obtained.

Nomenclature

A_j = jet cross-sectional area
C = circumference of jet cross section
C_D = crossflow drag coefficient of jet
C_p = pressure coefficient
d = length of major axis in elliptical representation of jet cross section
E_1,E_2,E_3 = entrainment coefficients
F_i = induced force
S = area of plate or finite wing
S_j = jet exhaust area
T = static thrust of jet
U = mainstream speed
U_j = jet speed
$\hat{\mathbf{V}}_j$ = unit jet exhaust vector
u,v,w = induced velocity components in X, Y, Z directions
X,Y,Z = coordinate system defined in Fig. 5a
X',Y',Z' = coordinate system defined in Fig. 5b
X_j,Y_j,Z_j = coordinates of jet exit in X, Y, Z coordinate system
X_p,Y_p,Z_p = coordinates of typical control point in X, Y, Z coordinate system
$\alpha_0,\beta_0,\gamma_0$ = mainstream flow direction cosines
ΔL = lift increment due to jet operation, $\Delta L = F_i + T$
δ_j = angle included between mainstream direction vector and jet exhaust vector
θ = angle defined in Fig. 1
ϕ,ψ = jet exhaust angles defined in Fig. 5a

Subscripts

0 = conditions at the jet exit
p = conditions at a control point

Superscripts

* = nondimensional value

Introduction

RECENTLY a number of configurations using lifting jets or fans have been considered which would provide an aircraft with V/STOL capability. An important consideration in a successful V/STOL design is the aerodynamic behavior of the aircraft. It is now well-known that during the transition phase, when the aircraft is not yet fully supported by the aerodynamic forces on the wing, as in conventional flight, there is a significant interference between the lifting jet efflux and the mainstream flow. This interference has a significant effect on the aerodynamics of the aircraft so that the performance, stability and control requirements of the aircraft are also affected. Consequently, in recent years there has been a considerable amount of research activity, aimed at clarifying these aerodynamic interference effects and developing methods for estimating the aerodynamic characteristics of lift jet and lift fan aircraft.

The first analytical approach to the problem of a jet exhausting into a crossflow was a purely potential flow model[1] which has recently been developed further.[2–4] This approach gives a good description of the jet cross section but calculations of the jet-induced flow do not correlate at all well with test data.[2] Another analytical approach assumes that the jet deflection is due to entrainment of crossflow fluid.[5] The entrainment of mainstream fluid is assumed to be due to two processes. The first is the usual entrainment process, observed in ordinary jets, arising from the presence of a mean velocity difference between the jet and the fluid into which it exhausts. The second mechanism results from the presence of the vortex pair into which the jet in a crossflow eventually degenerates. By allowing the entrainment coefficients to vary with velocity ratio and jet deflection angle, good correlation with test data was possible. However, the changes in the entrainment coefficients, which appear necessary to obtain this correlation, imply that the coefficients are not invariant and seem to preclude a generalization of this method.

A further approach assumed that the deflection of the jet is due to both entrainment of mainstream fluid into the jet and pressure forces on the boundary of the jet.[6] The continuity and momentum equations were integrated for the jet development, with values of the entrainment coefficients chosen to obtain correlation with test data. It was found that values of these coefficients could be determined which were invariant with change in velocity ratio. This method, as presented, was restricted to single jets exhausting normally into a crossflow out of the influence of ground effect. It is the purpose of this paper to extend this method to include the capability of calculations for multiple jets exhausting into an arbitrarily directed mainstream.

Single Jet Computations

Jet Model

The jet model assumes that the flow is incompressible and neglects viscous effects other than the entrainment caused by this mechanism. The entrainment of mainstream fluid into the jet and the pressure forces on the jet boundary govern the equations of motion, which can be written using the coordi-

Presented as Paper 70-545 at the AIAA Atmospheric Flight Mechanics Conference, May 13–15, 1970, Tullahoma, Tenn.; submitted June 1, 1970; revision received October 2, 1970. This work was supported by the Air Force Flight Dynamics Laboratory, Wright-Patterson Air Force Base, Ohio under contract F33615-69-C-1602.

* Senior Engineer, Research and Technology Department.
† Senior Technical Specialist, Research and Technology Department. Member AIAA.

nate system defined in Fig. 1:

continuity

$$\rho(d/ds)(A_jU_j) = E \tag{1}$$

momentum

$$\rho(d/ds)(A_jU_j^2) = EU\sin\theta \tag{2}$$

force

$$\begin{aligned}\rho A_jU_j^2/R &= EU\cos\theta + C_D\tfrac{1}{2}\rho U^2\cos^2\theta d \\ &= \rho A_jU_j^2X''/[1 + (X')^2]^{3/2}\end{aligned} \tag{3}$$

where the entrainment of mainstream fluid into unit length of the jet may be written

$$E = \rho E_1Ud\cos\theta + \rho E_2(U_j - U\sin\theta)C/1 + E_3U\cos\theta/U_j \tag{4}$$

A functional relationship between the cross-sectional area of the jet and the jet growth is established, based on experimental observations of the jet development. As shown in Fig. 1, an ellipse with a ratio of minor to major axis of $\frac{1}{4}$ is chosen to represent the kidney-shaped cross-sectional area into which a jet of initial circular cross section deforms according to experimental observations.[7] Experimental data further indicates that in the development region, in which the jet changes from a circular to an assumed elliptic cross section, the ratio of minor to major axis decreases linearly with distance from the jet orifice.[8]

After substitution of these geometric relationships into the equations of motion, a set of differential equations for U_j^*, d^*, X^* is obtained in terms of Z^*, the entrainment parameters and the crossflow drag coefficient. U_j^*, d^*, X^* are the mean jet velocity, jet diameter and the X-coordinate of the jet centerline in nondimensionalized forms.

Initial conditions at the jet exit are given as $Z^* = 0$, $X^* = 0$, $U_j^* = 1$, $d^* = 1$ and $dX^*/dZ^* = 0$. The equations of motion can now be integrated, with the entrainment coefficients and the crossflow drag coefficient chosen to obtain good correlation between the computed jet centerlines and test data.[7,9]

The jet-induced velocity field is obtained by replacing the jet by a sink-doublet singularity distribution. A distribution of uniform sinks along the axis normal to the oncoming mainstream accounts for the entrainment of mainstream fluid into the jet. The blockage effect of the jet is represented by a discrete doublet distribution on the centerline of the jet. From these sink and doublet distributions the jet-induced velocity components at a given control point can then be evaluated.

Integration of the Equations of Motion

The numerical integration of the equations of motion determining the growth and geometry of the jet was, in the original approach, performed by using a Taylor series expansion method. This integration procedure generated discernible differences in computed answers as a function of the integration step size. In an effort to reduce this variation of computed answers with integration step size, the system of first-order equations is now solved by means of a fourth-order Adams predictor/corrector method with a Runge-Kutta starting solution. For the integration intervals of Table 1 (utilizing an optimization capability to control integration step size within each interval), variation of the computed

Table 1 Effect of integration interval

Interval	U_j^*	d^*	X^*
0.2	0.302228	7.10419	4.29711
0.1	0.302214	7.10417	4.29728
0.05	0.302186	7.10382	4.29764

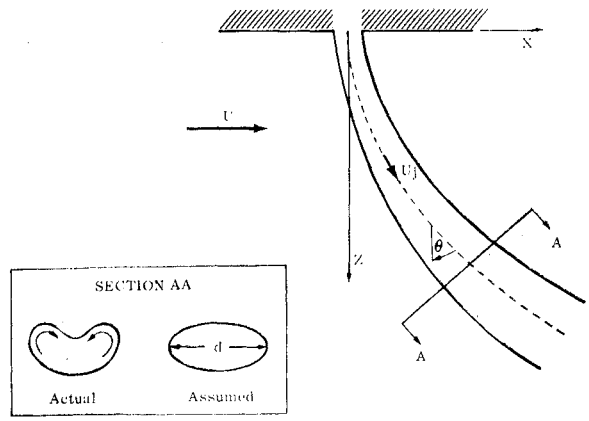

Fig. 1 Schematic of jet exhausting into crossflow.

variables U_j^*, d^* and X^* (all evaluated at $Z^* = 10$) is seen to be negligible.

Figure 2 shows the differences in computed jet centerlines due to the change in integration procedure, for jets exhausting normally into a crossflow at various velocity ratios, and provides a comparison with experimentally determined centerlines. The jet centerlines computed by using the predictor/corrector integration procedure are seen to exhibit a closer agreement with the test data.

The change in the numerical integration procedure also improved the correlation between computed pressures around an exhausting jet and experimental data. Figures 3 and 4 show the flat plate pressure distributions around a normally exhausting jet for velocity ratios of 8.0 and 11.3, respectively. Very good agreement between theory and experiment is evident for the velocity ratio of 11.3. The experimental data for the velocity ratio of 8.0 indicates that the theoretical results lie within experimental differences.[10,11]

Arbitrarily Directed Jet

Although the equations of motion for the jet model of Ref. 6 were written for jets exhausting normally into crossflows, they are valid for any jet in a local coordinate system, oriented with the X axis in the direction of the mainstream flow and the XZ plane defined by the mainstream flow vector and the jet exhaust vector. The direction of the mainstream, the location of the center as well as the initial direction of the exhausting jet, and the position of the points at which the induced velocity components are to be evaluated may be arbitrarily specified in a general, fixed coordinate system shown in Fig. 5a.

A local coordinate system centered at X_j, Y_j, Z_j is then established as shown in Fig. 5b. The direction cosines of $\hat{\mathbf{X}}'$ with respect to the fixed coordinate system are α_0, β_0, γ_0 and the direction cosines for $\hat{\mathbf{Y}}'$ and $\hat{\mathbf{Z}}'$ are determined from the following relationships

$$\mathbf{Y}' = \hat{\mathbf{V}}_j \times \hat{\mathbf{X}}'$$

$$\hat{\mathbf{Z}}' = \hat{\mathbf{X}}' \times \hat{\mathbf{Y}}'$$

where $\hat{\mathbf{V}}_j$ is the unit vector in the initial jet exhaust direction, obtained from ϕ and ψ, the jet exhaust angles.

This establishes the co-planar relationship between the mainstream flow and the jet centerline required by the equations of motion as formulated in Ref. 6. Initial conditions at the jet exit are now $Z^* = 0$, $X^* = 0$, $U_j^* = 1$, $d^* = 1$ and $dX^*/dZ^* = [(1 - \cos^2\theta)/\cos^2\theta]^{1/2}$ where $\cos\theta = \hat{\mathbf{V}}_j\cdot\hat{\mathbf{Z}}'$. The geometry of the developing jet and the jet-induced velocity components can then be computed in this local coordinate system, utilizing the equations developed in Ref. 6.

Computations were carried out for jets at various velocity ratios and deflection angles. A comparison of computed jet

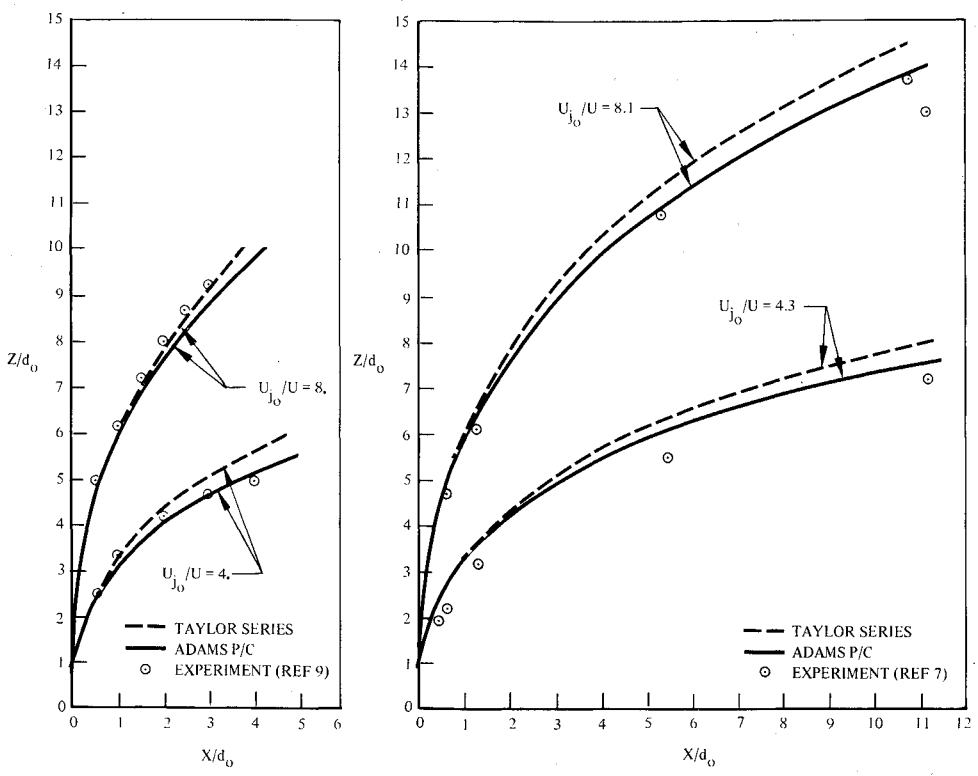

Fig. 2 Jet centerlines.

centerlines with an empirical equation for jets exhausting at angles other than 90° to the mainstream is shown in Figs. 6a–6d. They correspond to Figs. 12a, 13a, 14b, and 15a of Ref. 12. The solid curves represent centerlines computed for the specified conditions. The broken curves represent the empirical equation

$$X/d_0 = [-(U/U_{j0})^2/4 \sin^2\delta_j](Z/d_0)^3 - Z/d_0 \cot\delta_j \quad (5)$$

The curves superimposed on the photographs in Figs. 12–15 of Ref. 12 show the fit of this equation. It should be emphasized that the broken curves represent an empirical rather than experimental determination of the centerlines. They are included in Fig. 6 primarily to aid in orienting the computed centerlines with respect to the photographs of the jet wakes.

Figure 7 compares computed centerlines for a jet of velocity ratio 8.32 exhausting at various angles into the mainstream with test data.[5] Although agreement between theory and experiment is not as close as might be desirable, it should be noted that the computations were carried out employing values of the entrainment coefficients based on correlation with experimental data shown in Fig. 2. Comparison of the experimental centerline for the normally exhausting jet of Fig.

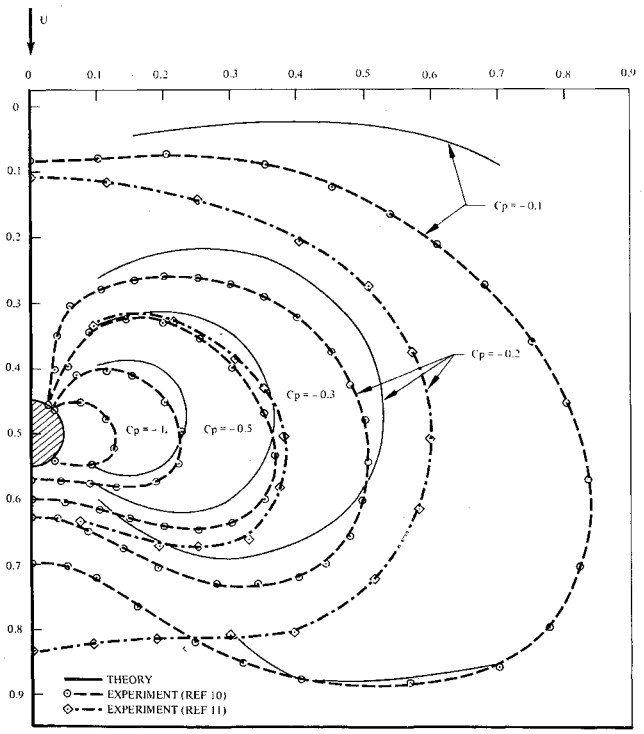

Fig. 3 Flat plate pressure distribution around a circular jet (U_{j0}/U = 8.0).

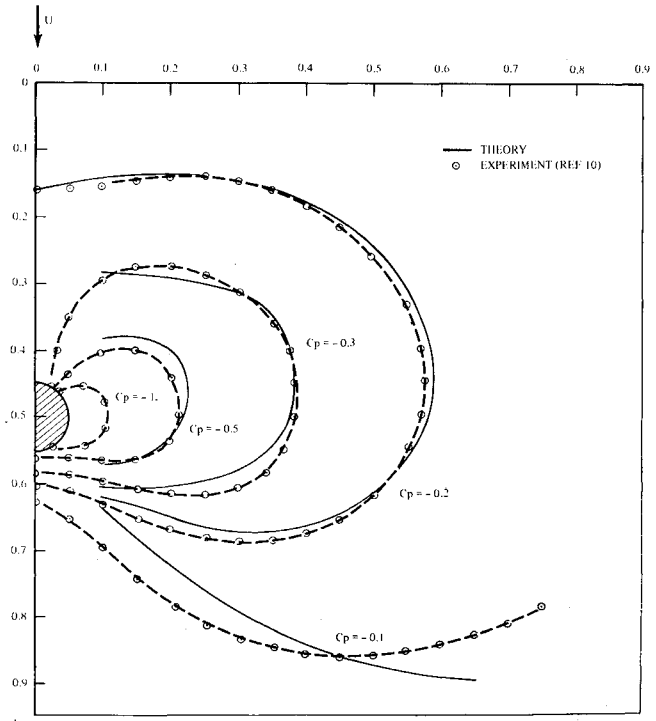

Fig. 4 Flat plate pressure distribution around a circular jet (U_{j0}/U = 11.3).

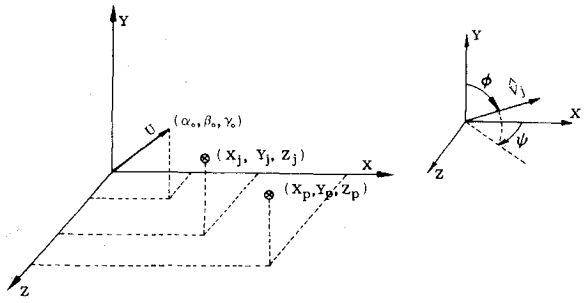

Fig. 5a General coordinate system.

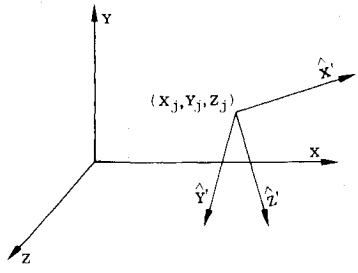

Fig. 5b Jet-centered coordinate system.

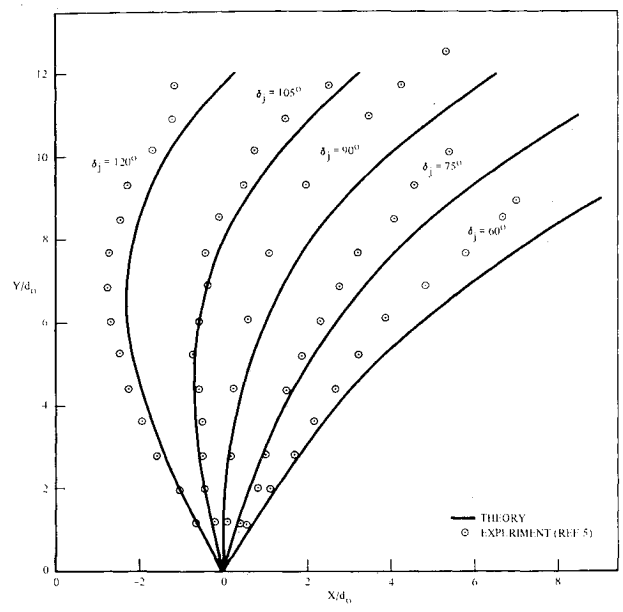

Fig. 7 Centerlines of a jet exhausting into a crossflow at various angles (U_{j0}/U = 8.32).

7 with the test data of Fig. 2a reveals differences which appear to be inconsistent with the small change in velocity ratio. In view of these experimental differences for the normally exhausting jet, the correlation for the other deflection angles shown in Fig. 7 is considered to be adequate.

A further comparison of theory with experiment for jets exhausting at an angle other than 90° is presented in Fig. 8. Good agreement of the computed results with the experimental data can again be observed.[18]

Figures 9 and 10 show the pressure distributions on a flat plate around a circular jet (U_{j0}/U = 8.) exhausting at angles of 60° and 120° into a crossflow. No experimental pressure determinations around jets exhausting at angles other than 90° to the mainstream were available for comparison.

Multiple Jet Computations

Figure 11 shows the planform of three jet configurations in relation to the mainstream flow. Arrangements a and c represent limiting cases. The arrangement a allows each of the two jets to develop independently to the point where the growth of each jet in the direction normal to the flow causes them to intersect. The configuration shown in c places the downstream jet entirely in the zone of influence of the upstream jet. The downstream jet is located partially in the zone of influence of the upstream jet in the arrangement depicted in b.

Although Fig. 11 shows the relationship of the jets in the plane of the jet exits, as an illustration, the determination of the degree of influence of the upstream jet (JET1) on the downstream jet (JET2) can be carried out for each increment of JET1 as shown in the general case, Fig. 12.

Plane L, defined by the mainstream flow vector and the diameter of JET1, identifies the increment of JET2 influenced by the increment of JET1. Plane M, which contains the mainstream flow vector and the local jet velocity vector of JET1, is then utilized in conjunction with the diameters of JET1 and JET2, to establish the extent to which the two jets overlap.

The influence of the upstream jet on the downstream jet is introduced into the computations as a reduced mainstream velocity in the continuity, momentum and force equations governing the development of the downstream jet. Equations (1–3), when applied to the downstream jet, now contain an effective mainstream velocity U_e in place of U where $U_e \leq U$. In the present formulation, a linear variation of

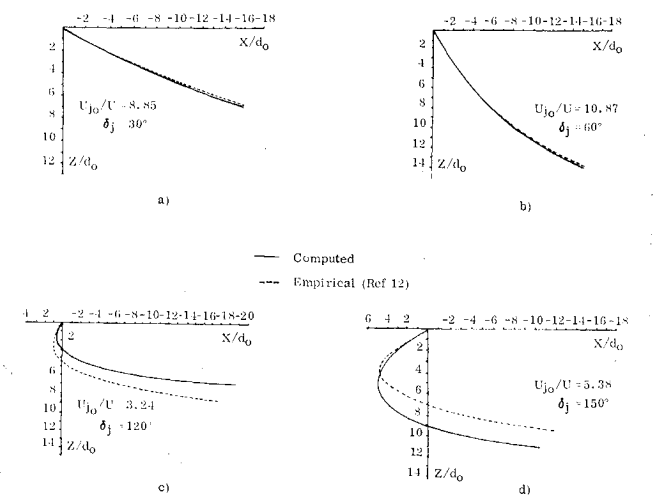

Fig. 6 Centerlines of jets exhausting into a crossflow at angles other than 90°.

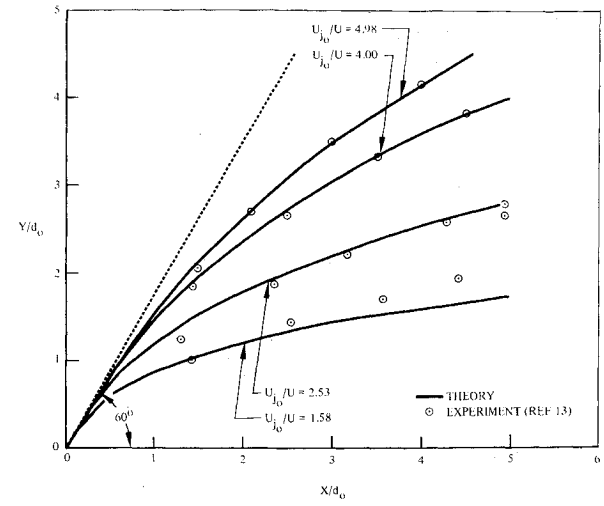

Fig. 8 Centerlines of jets exhausting into a crossflow at an angle δ_j = 60°.

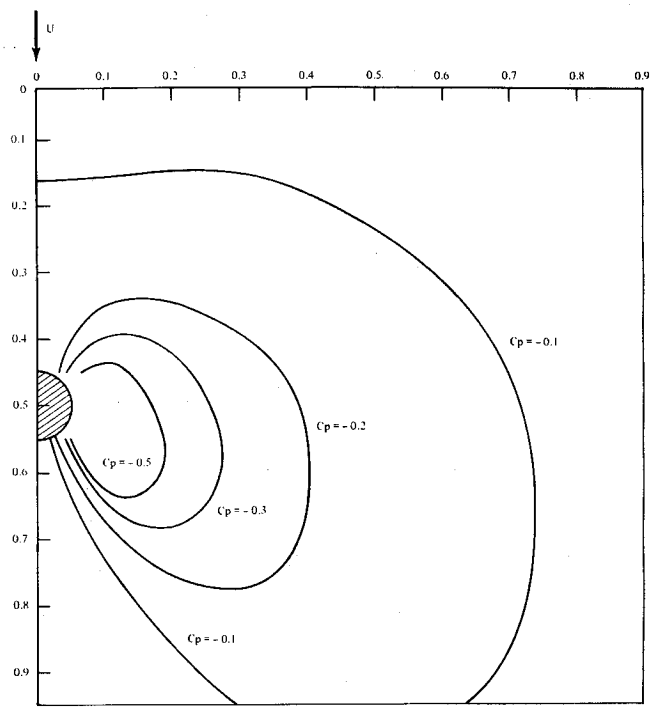

Fig. 9 Flat plate pressure distribution around a circular jet ($\delta_j = 60°$, $U_{j0}/U = 8.0$).

U_e/U with the extent to which the two jets overlap, as determined previously by the intersection of plane M, has been postulated. It has further been assumed that $U_e/U = 1.$ when there is no overlap between the two jets, and that $U_e/U = 0$ when JET1 overlaps JET2 completely. There does not appear to be any analytical justification for this relationship and test data, as it becomes available, will be instrumental in its proper definition.

Since the plane M is aligned with the mainstream flow vector as shown in Fig. 12, the minor axes of JET1 and JET2

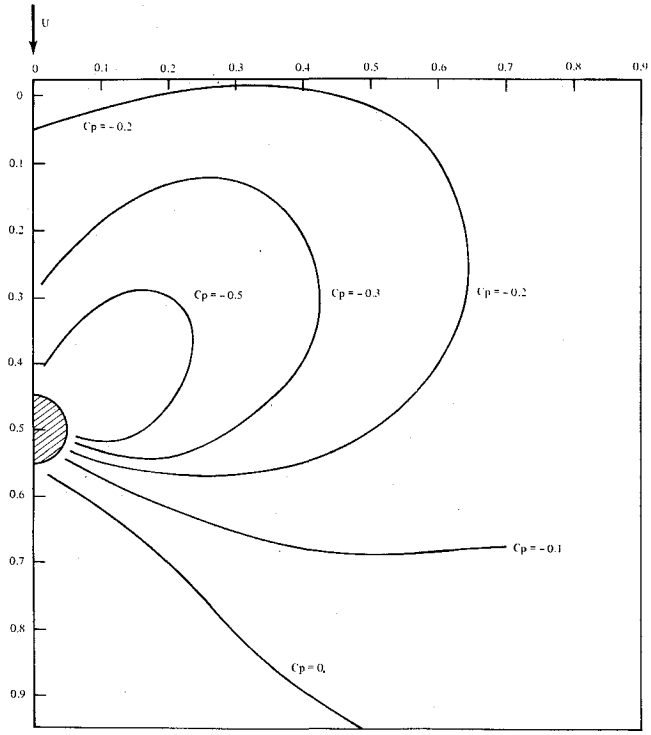

Fig. 10 Flat plate pressure distribution around a circular jet ($\delta_j = 120°$, $U_{j0}/U = 8.0$).

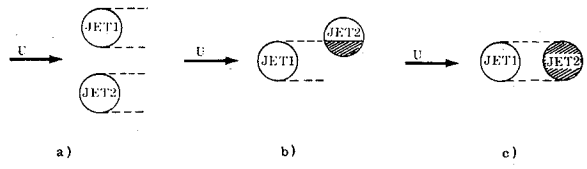

Fig. 11 Jet exit configurations.

also lie in this plane or a plane parallel to it. When computations show that there is overlap between the two jets, the normal distance between the major axes of JET1 and JET2 is computed. If the sum of the minor semiaxes of JET1 and JET2 is greater than this distance, intersection is assumed to have occurred. Initial conditions for the merged jet which results are determined from continuity and momentum considerations:

$$A_1U_{j1} + A_2U_{j2} = A_3U_{j3} \tag{6}$$

$$(A_1U_{j1})U_{j1x} + (A_2U_{j2})U_{j2x} = (A_3U_{j3})U_{j3x} \tag{7}$$

$$(A_1U_{j1})U_{j1y} + (A_2U_{j2})U_{j2y} = (A_3U_{j3})U_{j3y} \tag{8}$$

$$(A_1U_{j1})U_{j1z} + (A_2U_{j2})U_{j2z} = (A_3U_{j3})U_{j3z} \tag{9}$$

where A_1, A_2, A_3 = area of JET1, JET2 and resulting merged jet, respectively, and U_{j1}, U_{j2}, U_{j3} = jet velocities of JET1, JET2 and resulting merged jet, respectively.

Initial conditions for the merged jet, in the local coordinate system centered at the point of intersection of the two jets (taken to be an average of the coordinates of the centerlines of JET1 and JET2 at intersection), are $Z^* = 0$, $X^* = 0$, $U_j{}^* = 1$, $d^* = 1$, $dX^*/dZ^* = U_{j3x'}/U_{j3z'}$ and $U_{j03}/U = U_{j3}/U$. Subscripts x' and z' denote components in this local coordinate system.

These initial conditions are employed in integrating the set of differential equations for $U_j{}^*$, d^* and X^*. The cross-sectional area of this resultant jet is not circular, as is normally specified for an exhausting jet, but is assumed to be similar to the shape of the more developed of the two intersecting jets.

The velocity field induced by a given combination of jets can be determined by replacing each jet by its representative sink-doublet distribution. The induced velocity components, due to each sink-doublet distribution, are additive at every control point.

Computed centerlines for two jet arrangements of interest are shown in Figs. 13 and 14. The jets are all identical and exhaust normally into the crossflow.

The centerlines of two jets located at $X = 0.5$ and separated spanwise by three jet exit diameters are shown in Fig. 13. At $Z = -0.35$ the entrainment of crossflow fluid into the jets has caused the major axis of each jet to approach $3d_0$. This point, at which the two jets are assumed to merge, and the centerline of the resulting flow are indicated. The broken

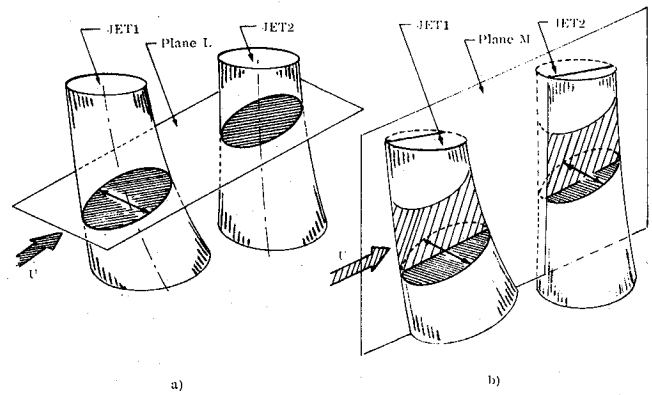

Fig. 12 Schematic of jet influence.

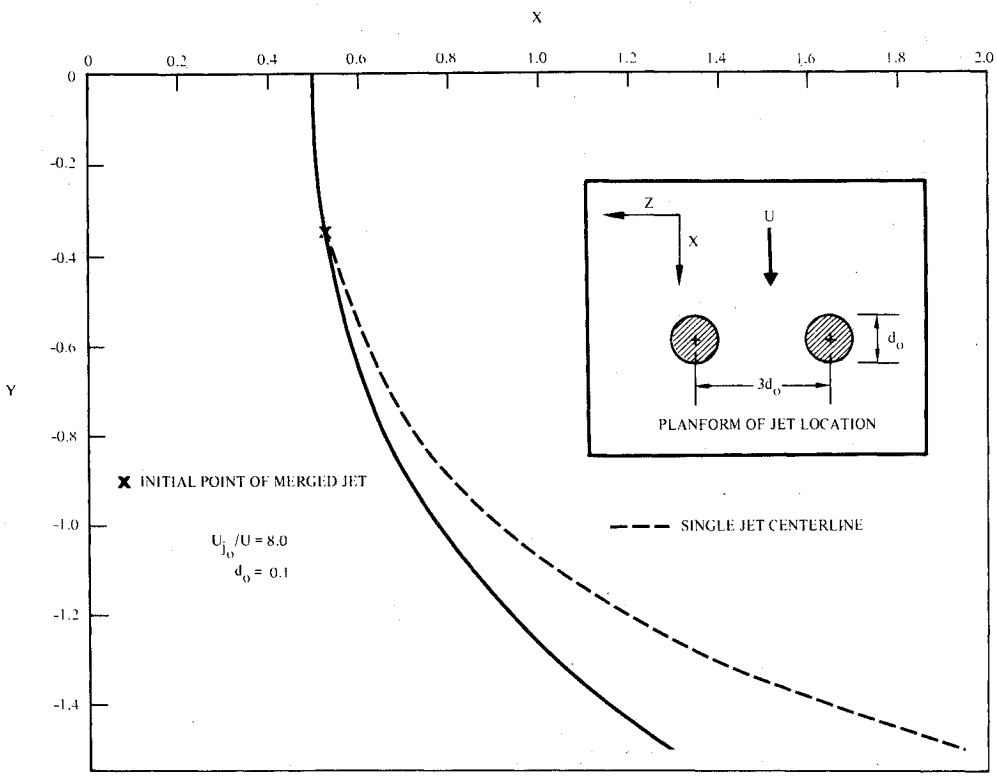

Fig. 13 Centerlines of two spanwise distributed jets exhausting normally into a crossflow.

curve, representing the computed centerline of a single jet located at $X = 0.5$, is included for comparison.

Figure 14 shows the centerlines of two chordwise distributed jets located at $X = 0.5$, $X = 0.8$. For these computations it was assumed that the chordwise jet distribution results in the complete screening of the downstream jet from the crossflow by the upstream jet (i.e., the downstream jet exhausts into a quiescent mainstream). At $Z = -0.6$ entrainment into the upstream jet has caused its major axis to increase to $4.4d_0$, with a minor semi-axis of $0.55d_0$. Entrainment into the downstream jet has resulted in a major axis of $2.9d_0$. Since the trailing jet, exhausting into a quiescent mainstream, retains a basically circular cross section, its minor semiaxis approaches $1.45d_0$. As the centerlines of the two jets are two jet exit diameters apart at this point, the criterion for intersection is satisfied. The centerline of the subsequent flow is again indicated, as is the centerline of a single jet, located at $X = 0.5$.

The analytical approach which has been illustrated requires that the planes defined by the mainstream flow vector and the jet exhaust vectors of the two jets be parallel. This restriction, adopted to simplify computations, in no way limits the applicability of the basic jet model to other configurations, while still encompassing most configurations of practical interest. The computational procedure, as illustrated for a two-

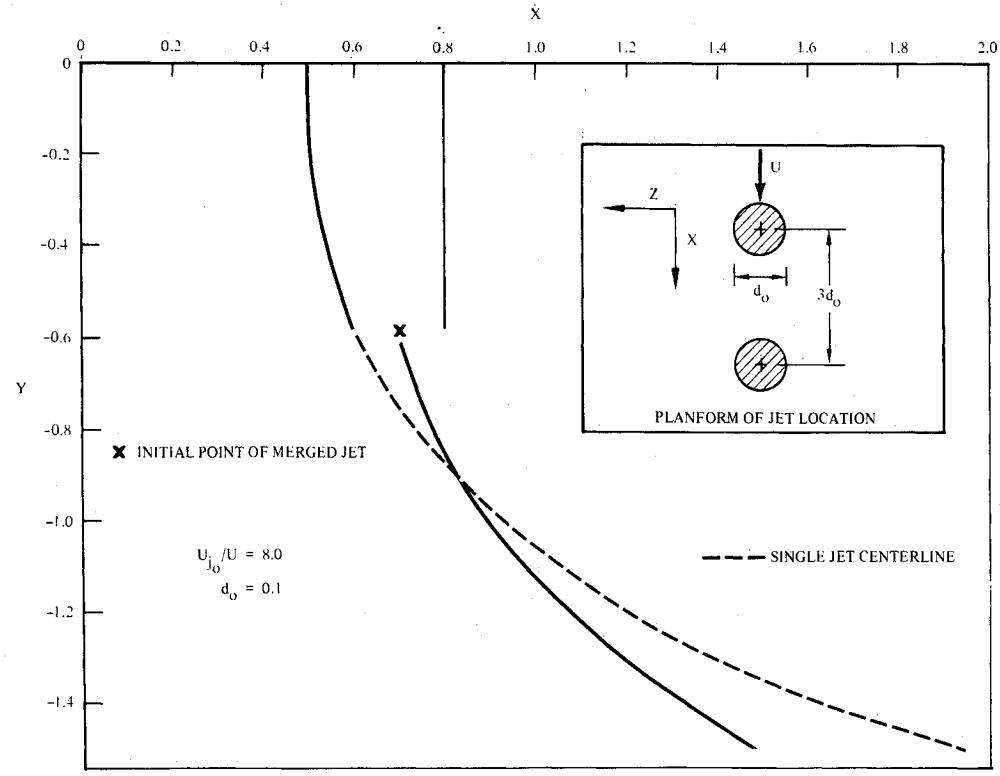

Fig. 14 Centerlines of two chordwise distributed jets exhausting normally into a crossflow.

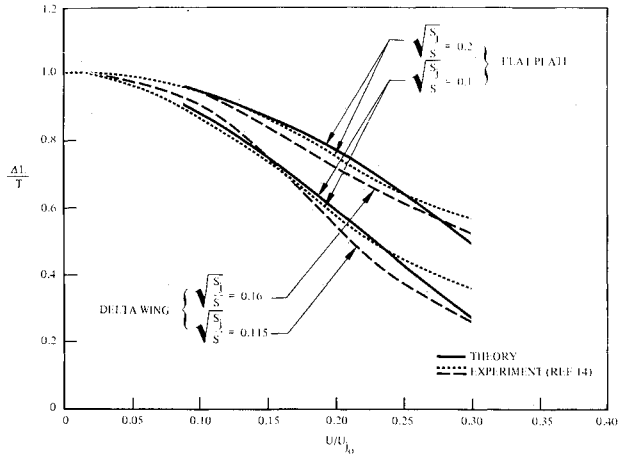

Fig. 15 Induced forces on flat plate and delta wing.

jet arrangement, can be applied to configurations involving more than two jets in a similar manner.

Applications

The basic model and the extensions delineated here are useful in computing flowfields due to jets exhausting into arbitrarily directed mainstreams.

The jet-induced velocity field may then be employed to explore the interaction between the given system of exhausting jets and adjacent supporting structures. Loading on an adjacent lifting surface may be predicted by lifting surface theory.

Integration of computed pressure coefficients to obtain total induced forces in the plane of the jet exit may be utilized in developing empirical relationships between these induced forces and moments and the velocity ratio of the exhausting jet. Figure 15 shows the computed variation of induced force on a flat plate around a normally exhausting jet with velocity ratio. Curves for the two values of the parameter $(S_j/S)^{1/2}$ are presented, where S_j is the jet exit area and S the portion of the flat plate over which the induced force is evaluated. Good correlation with the experimental data is discernible.[14] Experimental data on induced forces for delta wings with similar $(S_j/S)^{1/2}$ values indicate the utility of the model in estimating forces induced by exhausting jets on finite wings.

Conclusions

1) The jet model has proven to be very versatile in extending it to the treatment of arbitrary jet exhaust angles, arbitrary mainstream flow direction and multiple exhausting jets. 2) Available test data show good correlation with the theoretical calculations.

References

[1] Chang-Lu, H.-C., "Aufrollung eines zylindrischen Strahles durch Querwind," Doctoral dissertation, 1942, Univ. of Göttingen.

[2] Margason, R. J., *Analytical Description of Jet-Wake Cross Sections for a Jet Normal to a Subsonic Free Stream*, NASA SP-218, Sept. 1969.

[3] Braun, G. W. and McAllister, J. D., *Cross Wind Effects on Trajectory and Cross Sections of Turbulent Jets*, NASA SP-218, Sept. 1969.

[4] Hackett, J. E. and Miller, H. R., *The Aerodynamics of the Lifting Jet in a Cross Flowing Stream*, NASA SP-218, Sept. 1969.

[5] Platten, J. L. and Keffer, J. F., "Entrainment in Deflected Axisymmetric Jets at Various Angles to the Stream," Mechanical Engineering Rept. TP-6808, June 1968, Univ. of Toronto.

[6] Wooler, P. T., Burghart, G. H., and Gallagher, J. T., "Pressure Distribution on a Rectangular Wing with a Jet Exhausting Normally into an Airstream," *Journal of Aircraft*, Vol. 4, No. 6, Nov.–Dec. 1967, pp. 537–543.

[7] Jordinson, R., "Flow in a Jet Directed Normal to the Wind," R and M 3074, 1958, British Aeronautical Research Council.

[8] Abramovich, G. N., *The Theory of Turbulent Jets*, MIT Press, Cambridge, Mass., 1963, pp. 541–556.

[9] Keffer, J. F. and Baines, W. D., "The Round Turbulent Jet in a Cross Wind," *Journal of Fluid Mechanics*, Vol. 15, 1963, pp. 481–496.

[10] Bradbury, L. J. S. and Wood, M. N., "The Static Pressure Distribution Around a Circular Jet Exhausting Normally from a Plane Wall into an Airstream," TN AERO 2978, Aug. 1968, Royal Aircraft Establishment.

[11] Gelb, G. H. and Martin, W. A., "An Experimental Investigation of the Flow Field About a Subsonic Jet Exhausting into a Quiescent and a Low Velocity Airstream," *Canadian Aeronautics and Space Journal*, Vol. 12, No. 8, Oct. 1966, pp. 333–342.

[12] Margason, R. J., "The Path of a Jet Directed at Large Angles to a Subsonic Free Stream," TN D-4919, 1968, NASA.

[13] Shandorov, G. S., "Calculation of the Axis of a Jet in a Cross Flow," *Soviet Aeronautics*, Vol. 9, No. 2, 1969, pp. 60–62.

[14] Williams, J. and Wood; M. N., "Aerodynamic Interference Effects with Jet-Lift V/STOL Aircraft under Static and Forward-Speed Conditions," TR 66403, Dec. 1966, Royal Aircraft Establishment.